Available online at www.sciencedirect.com
SCIENCE DIRECT®
Journal of Solid State Chemistry 177 (2004) 1230–1234
JOURNAL OF SOLID STATE CHEMISTRY
http://elsevier.com/locate/jssc

Synthesis of metastable hexagonal In_2O_3 nanocrystals by a precursor-dehydration route under ambient pressure

Dabin Yu, Debao Wang, and Yitai Qian*

Structure Research Lab, Department of Chemistry, University of Science and Technology of China, Hefei Anhui, 230026, People's Republic of China

Received 4 August 2003; received in revised form 19 October 2003; accepted 29 October 2003

Abstract

Single-crystalline metastable In_2O_3 nanocrystals with size in the range of 5–30 nm were, for the first time, synthesized by a precursor-dehydration route at 490°C under ambient pressure. The precursor was prepared by a hydrolysis solvothermal reaction using $InCl_3 \cdot 4H_2O$ as starting materials and ethylenediamine as solvent in the range of 180–230°C. It was found that the precursor had significant effect on the phase composition and phase structure of In_2O_3. Optical properties of the metastable In_2O_3 nanocrystals were investigated.

Keywords: Metastable In_2O_3; Nanocrystals; Precursor-dehydration route; Solvothermal reaction

1. Introduction

Due to the high electrical conductivity and good optical transparency [1], In_2O_3 has attracted considerable research interest for several decades. It has been widely used in optoelectronic devices such as solar cells, liquid crystal displays and gas sensors, and in particular it has shown remarkable potential applications in the upcoming nanoelectronic building blocks and nanosensors [2–6]. To satisfy the requirements of the wide applications of In_2O_3, many fabrication techniques such as thermal decomposition of precursors [7,8], sol–gel method [9], chemical vapor deposition [10], and dc magnetron sputtering [11] have been successfully developed. However, various In_2O_3 products including powders [12], nanocrystallites [4,13], and thin films [14] fabricated by these techniques were predominantly the low-pressure form with bixbyite structure (JCPDS 6-0416), while the pure metastable In_2O_3 with corundum structure, the so-called high-pressure phase, has seldom been related [15,16].

Previously, metastable In_2O_3 was synthesized by phase transition methods under the conditions of high pressure and/or high temperature. Shannon reported the high-pressure transformation of In_2O_3 to a modification with the corundum structure [17]. Thereafter, Prewitt et al. prepared metastable In_2O_3 at 65 kbars and 1100°C [15]. Atou et al. synthesized metastable In_2O_3 under pressure of 15–25 GPa by shock-induced phase transition method [18]. It had not been synthesized under ambient pressure in particular by a chemical approach until we successfully synthesized the metastable hexagonal In_2O_3 nanofibers [19].

Recently, based on our previous work, we found that well-crystallized InOOH or its hydrate in nanometer size was a key factor for the formation of the metastable In_2O_3 nanocrystals. In this paper, we report the synthesis of metastable In_2O_3 nanocrystals by a precursor-dehydration route under ambient pressure at 490°C. The precursor was prepared by the hydrolysis of In^{3+} using $InCl_3 \cdot 4H_2O$ and deionized water as starting materials and using ethylenediamine as solvent in the range of 180–230°C. The effect of the precursor on the phases of the final products was investigated. Besides, optical properties of the as-synthesized metastable In_2O_3 nanocrystals were also studied.

2. Experimental section

All of the solvents and reagents were of analytical purity. In a typical procedure, 1.50 g $InCl_3 \cdot 4H_2O$ and 2–3 mL deionized water were put into a Teflon-lined

*Corresponding author. Fax: +86-551-360-7402.
E-mail addresses: dabinyu@mail.ustc.edu.cn (D. Yu), ytqian@ustc.edu.cn (Y. Qian).

0022-4596/$ - see front matter © 2003 Elsevier Inc. All rights reserved.
doi:10.1016/j.jssc.2003.10.030

stainless steel autoclave of 50 mL capacity. After $InCl_3 \cdot 4H_2O$ had dissolved, 40 mL ethylenediamine was added into the autoclave. Immediately, a floccule-like precipitate was obtained, and it was dispersed ultrasonically in ethylenediamine. Then, the autoclave was sealed and heated at 180–230°C for 24 h, then cooled to room temperature naturally. The sample was filtered and washed several times with absolute ethanol and distilled water, respectively. After being dried in vacuum, the precursor was obtained. Metastable In_2O_3 nanocrystals were prepared by putting the precursor in a quartz crucible and annealing in a furnace at 490 °C under ambient pressure for 2 h [19].

X-ray powder diffraction (XRD) patterns were recorded on a Japan MAC SCIENCE MXP18AHF X-ray diffractometer ($\lambda = 1.54056$ Å). Transmission electron microscopy (TEM) images were taken with a Hitachi model H-800 transmission electron microscope, using an accelerating voltage of 200 kV. High-resolution transmission electron microscopy (HRTEM) image, selected area electron diffraction (SAED), and energy dispersive spectra (EDS) of the samples were obtained on a JEOL-2010 TEM with an attached EDS system at an acceleration voltage of 200 kV. Elemental analysis was preformed with a VARIO ELIII elemental analyzer at 850°C in O_2. The X-ray photoelectron spectra (XPS) were recorded on an ESCALab MK X-ray photoelectron spectrometer, using Al $K\alpha$ radiation as the exiting source. Optical absorption spectra were determined on a UV-2401PC UV/Vis recording spectrophotometer, and the metastable In_2O_3 nanocrystals were ultrasonically dispersed in absolute ethanol for the measurement.

3. Results and discussion

The synthesis was based on the following reactions:

$$In^{3+} + 3H_2O \rightarrow In(OH)_3 + 3H^+ \quad (1)$$

$$In(OH)_3 \rightarrow InOOH + H_2O \quad (2)$$

$$2InOOH \rightarrow In_2O_3 + H_2O \quad (3)$$

With the addition of ethylenediamine into the $InCl_3$ solution, the reaction (1) took place immediately resulting in the formation of the floccule-like precipitate. Under heating condition, the precipitate dehydrated to form the precursor, InOOH or its hydrate, during which the reaction (2) took place. When the annealing temperature was higher than 485°C, the precursor could completely dehydrate to form metastable In_2O_3, as described in reaction (3) [19].

Both the temperature and solvent played crucial role in the preparation of the precursor. The suitable temperature for the preparation of precursor was 180–230°C, while the precursors obtained at different temperatures had different chemical composition. When the temperature was lower than 200°C, the precursor was the hydrate of InOOH, which was also found to be an effective precursor for the formation of the metastable In_2O_3 nanocrystals in our recent work. Fig. 1a shows a typical XRD pattern of the precursor prepared at 190°C. Most of the peaks can be indexed to orthorhombic InOOH with cell parameters of $a = 5.288$ Å, $b = 4.587$ Å and $c = 3.248$ Å in agreement with literature (JCPDS No. 17-549), while several other peaks marked with triangles are unidentified according to JCPDS cards. This precursor was further analysed by XPS (see Fig. 2), indicating the precursor is only composed of In and O. Since H cannot be detected by XPS, its content in the precursor is determined by elemental analysis, indicating that there was ca. 1.6 wt% H. So the precursor can be considered as a hydrate of InOOH, $InOOH \cdot 0.75H_2O$. When the temperature was higher than 210°C, such as at 220°C, the precursor was a pure phase of nanocrystalline InOOH as shown in Fig. 1b, in which all the peaks can be indexed to orthorhombic InOOH (JCPDS No. 17-549), which is similar to the preparation of InOOH nanofibers in ether at 230°C [19]. The difference of the precursors obtained at different temperatures was due to the unstable thermal property of $InOOH \cdot xH_2O$, which could dehydrate at a higher temperature resulting in the formation of a pure phase of InOOH. The sharp and strong peaks of the XRD patterns indicate that the precursor, InOOH or its hydrate, was well crystallized, while the wide peaks indicate that the as-prepared precursors have small particles in nanometer size according to the Scherer equation [20]. The well-crystallized precursors in nanometer size are crucial for

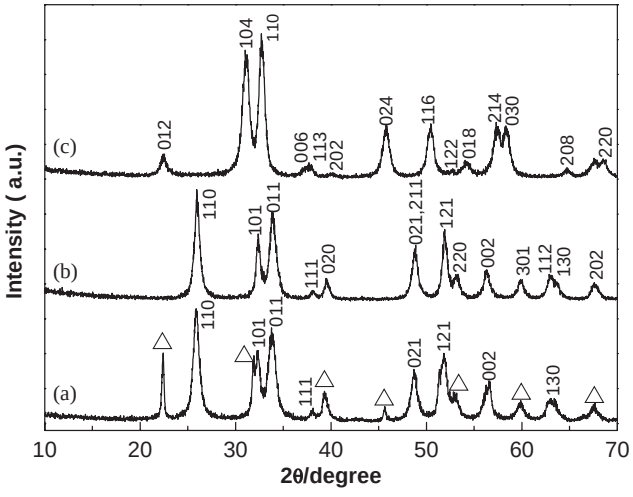

Fig. 1. XRD patterns of: (a) the precursor prepared at 190°C, most of the peaks can be indexed to orthorhombic InOOH, while several other peaks marked with triangles are unidentified according to JCPDS cards; (b) the precursor prepared at 220°C; and (c) the precursors annealed at 490°C for 2 h, all of the peaks can be indexed to the metastable In_2O_3 with corundum structure.

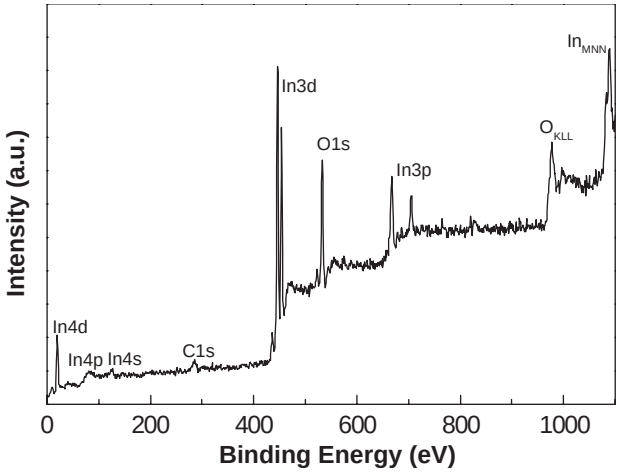

Fig. 2. X-ray photoelectron spectroscopy (XPS) of the precursor as related in Fig. 1a.

Table 1
The experimental observed d-spacings of the metastable In_2O_3 nanocrystals and those reported in JCPDS No. 22-336

hkl	d_{obs}/Å	d_{Ref}/Å
012	3.976	3.970
104	2.882	2.883
110	2.741	2.743
006	2.420	2.418
113	2.384	2.387
202	2.257	2.258
024	1.989	1.987
116	1.812	1.814
122	1.744	1.743
018	1.693	1.694
214	1.608	1.609
030	1.583	1.584
208	1.442	1.441
220	1.371	1.371

Note: $a = 5.484$ Å and $c = 14.508$ Å.

the formation of the metastable In_2O_3 nanocrystals, which will be discussed in the following paragraphs. The solvent mainly affected the morphology of the precursor, which further determined the morphology of the final product by template action [7,19]. Unlike the precursor prepared in ether [19], the precursor prepared in ethylenediamine was nearly spherical particles, however, the basic solvent was favorable for the hydrolysis of In^{3+} thus resulting in high yield of the products (>95%) so that this was a very effective route.

Fig. 1c shows a typical XRD pattern of the final products obtained by annealing the precursors at 490°C under ambient pressure, in which all the peaks can be indexed to metastable In_2O_3 with corundum structure (JCPDS, No. 22-336). The strong and sharp peaks indicate that the sample is well crystallized. The lattice parameters of the as-prepared In_2O_3 are $a = 5.484$ Å and $c = 14.508$ Å (CELL. Ver. 5.0, copyright 1986 by K. Dwight), which are good in consistent with the reported values of $a = 5.487$ Å and $c = 14.510$ Å at 65 kbars (Table 1) (JCPDS, No. 22-336). The chemical composition was further investigated by EDS, indicating that the final product consisted of In and O in a molar ratio of ca. 2:3, without other elements that could be detected within the sensitivity of the apparatuses.

Fig. 3a shows a typical TEM image of the final products, indicating that the sample is particles with average diameter of ca. 15 nm and with spherical morphology. A typical ED pattern is shown in Fig. 3b. All of the electron diffraction rings can be indexed to the metastable In_2O_3, which is in good agreement with the XRD analysis. The HRTEM image (see Fig. 3c) clearly shows that each particle has identical lattices fringes, indicating that individual nanoparticle is a single crystal. The fringe spacing of the nanocrystal in the middle of the image is estimated to be 0.378 nm, which is close to the (012) lattice spacing of metastable In_2O_3. Therefore, as described all above, the final products are the single-crystalline nanocrystals of pure metastable In_2O_3.

In order to investigate the effect of the precursor on the phase of the final products, various precursors have been used to synthesize In_2O_3 by the same annealing process. It was found that the well-crystallized InOOH or its hydrate is pivotal for the formation of the metastable In_2O_3. For instance, if the floccule-like precipitate of $In(OH)_3$ (amorphous form) or its nanocrystallites (crystal form) were used as precursor, only cubic In_2O_3 crystals could be obtained (see Fig. 4a). This was similar to the sol–gel method that was usually used for the fabrication of In_2O_3 [9,21]. If the reaction time was short or the temperature was not high enough in the solvothermal process, the obtained precursor was not well crystallized or the floccule-like precipitate did not react completely, after the same annealing process, the final product was the mixture phases of hexagonal and cubic In_2O_3 (see Fig. 4b). These indicated that the chemical composition and crystallization of the precursor had significant effect on the phase composition and phase structure of final products. On the other hand, from both the kinetics and the stability point of view, the metastable materials could be more easily achieved in nanocrystals than in large crystals (bulk) under ambient pressure [22,23]. In this regard, the as-prepared precursors in nanometer size were favorable for the formation of the metastable In_2O_3 nanocrystals since it has been proved that the precursors acted as template for the formation of the metastable In_2O_3 nanocrystals [19]. Since solvothermal reactions were carried out at a favorable pressure [24,25], the well-crystallized precursor, nanocrystalline InOOH or its hydrate, could be easily achieved. Thus, on the base of the precursor, metastable In_2O_3 nanocrystals were successfully synthesized under ambient pressure.

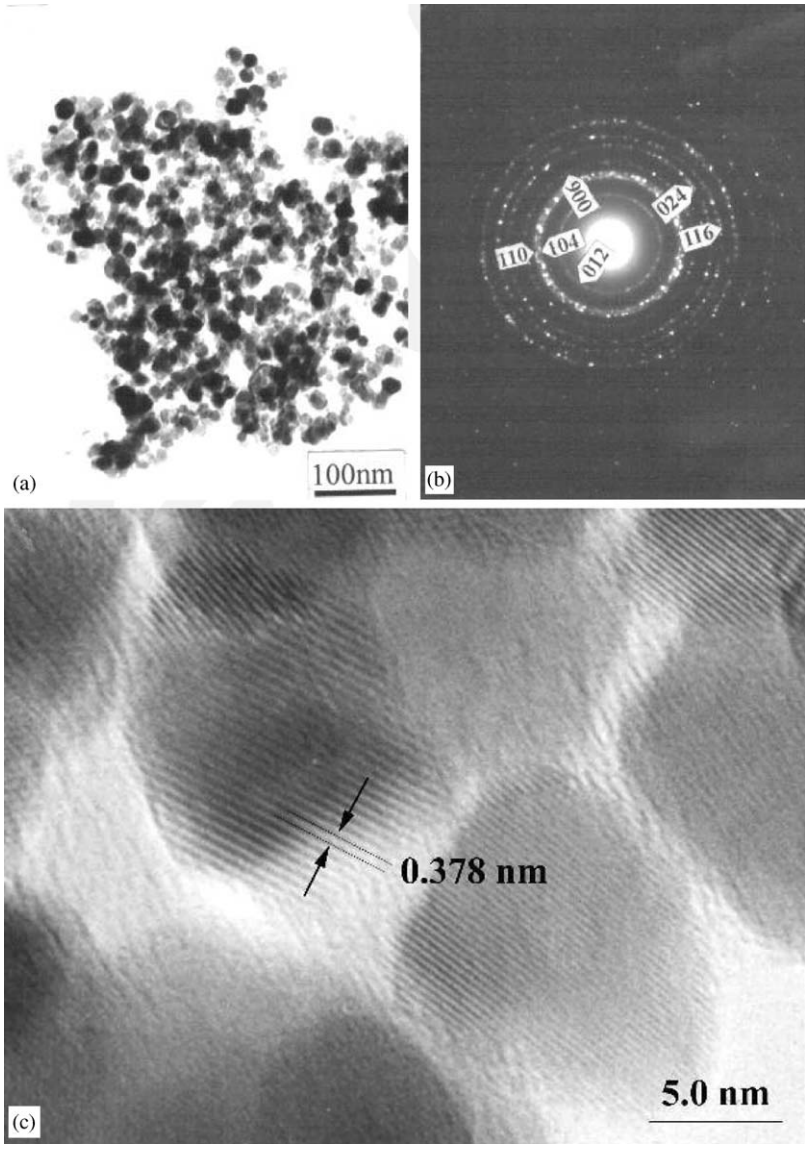

Fig. 3. (a) TEM image with the magnifications of 1×10^5, (b) ED pattern, and (c) HRTEM image of the metastable In_2O_3 nanocrystals.

Fig. 5 shows the absorption spectra of metastable In_2O_3 nanocrystals with different average particle size of 28, 15, and 7 nm, respectively. It can be clearly seen that there is no absorption peaks in the whole visible region, but there is strong absorption in the UV region. This is due to the wide band gap of In_2O_3, which has been reported to be 3.75 eV [26], where the bottom of the conduction gap is the metal 5*s* band and the top of the valence band is the O^{2-}: $2p^6$ band. The spectra also indicate the evolution of the optical spectra with the change of particle size. It can be seen that the absorption edges, characteristic peaks, and tails in the spectra shifted towards the shorter wavelength with the decrease of particle size, probably resulting from quantum effect [9]. Optical band gap was calculated from the absorption coefficient data by plotting α^2 vs. E and extrapolating the linear portion of the curve to $\alpha^2 = 0$, where α is the absorption coefficient and E is the photon energy. Consequently, the band gaps of samples *a*, *b*, and *c* were 3.80, 3.85, and 3.96 eV, respectively, exhibiting slightly blue sift in comparison with that of bulk In_2O_3 (3.75 eV) with the decrease of particle size, while the data are still close to those reported data of In_2O_3 with bixbyite structure (3.5–3.9 eV) [10,27]. Compared with the optical spectra of the In_2O_3 with bixbyite structure [14,27], the spectra indicate that the metastable In_2O_3 nanocrystals also have the possibility of high optical transparency in a wide visible region, thus have the potential applications in optoelectronic devices.

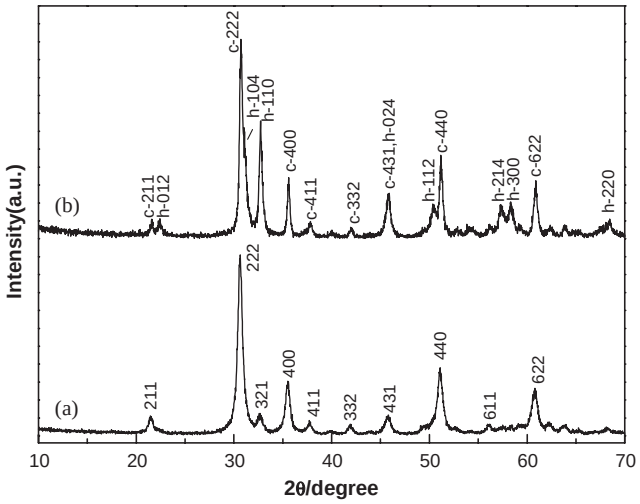

Fig. 4. XRD patterns: (a) all of the peaks can be indexed to cubic In_2O_3; and (b) the peaks marked with "c" can be indexed to cubic In_2O_3, while those marked with "h" can be indexed to hexagonal metastable In_2O_3.

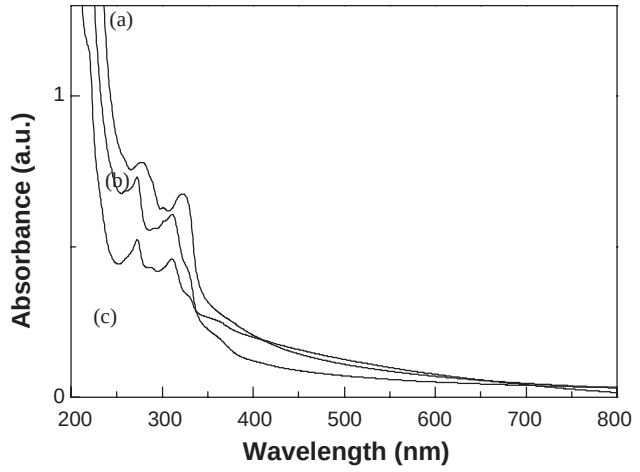

Fig. 5. Optical absorption spectra of the metastable In_2O_3 nanocrystals with different average particle size: (a) 28 nm, (b) 15 nm, and (c) 7 nm.

4. Conclusion

Pure In_2O_3 nanocrystals of the high-pressure phase with corundum structure have been prepared at a relatively low temperature and under ambient pressure. The UV/vis absorption spectra indicated that the In_2O_3 nanocrystals had the possibility of high optical transparency in a wide visible region. Although more investigations are still needed, we believe in principle that this is a practical approach to the high-pressure phase of In_2O_3, and also an effective route to metal-doped In_2O_3 such as ITO (tin-doped In_2O_3) with corundum structure. Moreover, our results show a successful example for the preparation of the metastable semiconductor nanocrystals under relatively mild conditions.

Acknowledgments

We gratefully acknowledge the National Science Foundation of China and Science Foundation of Anhui Province (No. 03044903) for financial support.

References

[1] C.G. Granqvist, Appl. Phys. 57 (1993) 19.
[2] H. Zhou, W. Cai, L. Zhang, Appl. Phys. Lett. 75 (1999) 495.
[3] A. Gurlo, M. Ivanovskaya, N. Bârsan, M. Schweizer-Berberich, U. Weimar, W. Göpel, A. Diéguez, Sensor. Actuat. B 44 (1997) 327.
[4] K. Soulantica, L. Erades, M. Sauvan, F. Senocq, A. Maisonnat, B. Chaudret, Adv. Funct. Mater. 13 (2003) 553.
[5] C. Li, D.H. Zhang, X.L. Liu, S. Han, T. Tang, J. Han, C.W. Zhou, Appl. Phys. Lett. 82 (2003) 1613.
[6] D.H. Zhang, C. Li, S. Han, X.L. Liu, T. Tang, W. Jin, C.W. Zhou, Appl. Phys. Lett. 82 (2003) 112.
[7] N. Audebrand, J.P. Anffredic, D. Louër, Chem. Mater. 10 (1998) 2450.
[8] N. Audebrand, S. Raite, D. Louër, Solid State Sci. 5 (2003) 783.
[9] R.B.H. Tahar, T. Ban, Y. Ohya, Y. Takahashi, J. Appl. Phys. 82 (1997) 865.
[10] S. Suh, D.M. Hoffman, J. Am. Chem. Soc. 122 (2000) 9396.
[11] Y. Shigesato, D.C. Paine, Thin Solid Films 238 (1994) 44.
[12] S.K. Poznyak, A.N. Golubev, A.I. Kulak, Surf. Sci. 454 (2000) 396.
[13] M. Zhang, L. Zhang, X. Zhang, J. Zhang, G. Li, Chem. Phys. Lett. 334 (2001) 298.
[14] J.S. Cho, K.H. Yoon, S.K. Koh, Thin Solid Films 368 (2000) 111.
[15] C.T. Prewitt, R.D. Shannon, D.B. Rogers, A.W. Sleight, Inorg. Chem. 8 (1969) 1985.
[16] J.D.H. Donnay, H.M. Ondik, Crystal Data Determinative Tables, Vol. II, Inorganic Compounds, 3rd Edition (H-255, 2.6444), USA, 1973.
[17] R.D. Shannon, Solid State Commun. 4 (1966) 629.
[18] T. Atou, K. Kusaba, K. Fukuoka, M. Kikuchi, Y. Syono, J. Solid State Chem. 89 (1990) 378.
[19] D.B. Yu, S.H. Yu, S.Y. Zhang, J. Zuo, D.B. Wang, Y.T. Qian, Adv. Funct. Mater. 13 (6) (2003) 497.
[20] H.P. Klug, L.E. Alexaner, X-ray Diffraction Procedure for Polycrystalline and Amorphous Materials, 2nd Edition, Wiley Press, New York, 1974.
[21] S.S. Kim, S.Y. Choi, C.G. Park, H.W. Jin, Thin Solid Films 347 (1999) 155.
[22] C.-C. Chen, A.B. Herhold, C.S. Johnson, A.P. Alivisatos, Science 276 (1997) 398.
[23] Y. Xie, Y. Qian, W. Wang, S. Zhang, Y. Zhang, Science 272 (1996) 1926.
[24] Y.T. Qian, Adv. Mater. 11 (1999) 1101.
[25] K.B. Tang, Y.T. Qian, J.H. Zeng, X.G. Yang, Adv. Mater. 15 (2003) 448.
[26] I. Hamberg, C.G. Granqvist, Sol. Energy Mater. 14 (1986) 241.
[27] L.A. Ryabova, V.S. Salun, I.A. Serbinov, Thin Solid Films 92 (1982) 327.